Computer-assisted Ultrasound Assessment of Plaque Characteristics in Radiation-induced and Non-radiation-induced Carotid Atherosclerosis

Yuanxi Li
Hong Kong Polytechnic University
Dora LW Kwong
University of Hong Kong
Vincent WC Wu
Hong Kong Polytechnic University
Shea-Ping Yip
Hong Kong Polytechnic University
Helen KW Law
Hong Kong Polytechnic University
Shara WY Lee
Hong Kong Polytechnic University
Michael Ying (michael.ying@polyu.edu.hk)
Hong Kong Polytechnic University https://orcid.org/0000-0001-5979-6072

Original investigation

Keywords: carotid atherosclerosis, carotid plaque texture, subclinical atherosclerosis, radiation effects, ultrasound

Posted Date: April 7th, 2020

DOI: https://doi.org/10.21203/rs.3.rs-20336/v1

Abstract

Background Carotid atherosclerosis is common in post-radiotherapy (post-RT) patients and subjects with cardiovascular risk factors (CVRFs). The associated development of carotid plaques (CPs), particularly unstable plaques, is a major cause of cerebrovascular disease. Therefore, accurate detection and evaluation of CP characteristics is of essence. This study investigated the feasibility of using a computer-assisted method to evaluate and differentiate the CP characteristics in radiation-induced and non-radiation-induced CA. Methods 107 post-RT NPC and 110 CVRF subjects were recruited. Each participant had a carotid ultrasound examination of CPs and carotid intima-media thickness (CIMT). The carotid plaque characteristics were evaluated for grey-scale median (GSM) and detailed plaque texture analysis (DPTA) using specific computer software. In DPTA, five different intra-plaque components were color-coded according to different grey scale ranges. Multivariate regression model was used to evaluate the correlation of risk factors and carotid plaque characteristics. Results Post-RT NPC patients have significantly higher CIMT (748±15.1μm, p=0.001), more incidence of plaque formation (80.4%, p<0.001) and larger number of plaques (2.3±0.2, p<0.001) than CVRF subjects (680.4±10.0μm, 38.2% and 0.5±0.1 respectively). Among the five intra-plaque components, radiation-induced carotid plaques had significantly larger area of calcification (4.8 ±7.7%, p=0.012), but lesser area of lipid (42.1%±16.9%, p=0.034) when compared to non-radiation-induced CPs (3.0%±5.7% and 46.3%±17.9% respectively). Age, radiation and number of CVRF were significantly associated with the CA burden (p<0.001). Besides, age was significantly associated with the amount of lipid and calcification within CPs (p<0.001). Conclusions Compared to CVRF subjects, post-RT NPC patients were more susceptible to carotid plaque formation with less lipid content. Considering both CA burden and plaque component, both post-RT NPC patients and individuals with CVRF have a high risk of cerebrovascular diseases.

Background

Nasopharyngeal carcinoma (NPC) is a common head and neck cancer in Southeast Asia. There were 129,079 new cases globally(1) in 2018, and Southeast Asia possessed the top nine countries with the highest incidence of new NPC cases. Nodal metastasis is common in NPC patients, with about 60–90% of the patients having neck lymph node metastasis. Radiotherapy (RT) is the common treatment for both the primary tumour and metastatic neck lymph nodes for NPC, and chemotherapy may be used in conjunction with RT for patients in advanced disease stages(2). Since extracranial carotid arteries are in close proximity to neck lymph nodes, they are unavoidably irradiated during the RT of neck lymph nodes(3, 4). Carotid atherosclerosis (CA) is a late post-RT complication in patients who received external irradiation to head and neck. It is a chronic inflammatory disease, which is identified by the increased carotid intima-media thickness (CIMT) and the formation of carotid atherosclerotic plaque(5, 6) subclinically. Due to the progressive property of CA development, different characteristics of plaques could represent different stages of atherosclerosis. Atherosclerosis is well-accepted to be initiated by the endothelial dysfunction on the surface of blood vessel wall. The injured endothelium elicits the sub-endothelial accumulation of cholesterol, namely oxidized low-density lipoprotein. Monocyte-derived

macrophages and lymphocytes are then recruited at the intima, resulting in the formation of foam cells. Meanwhile, smooth muscle cells migrate from the media and are recruited at the lesion site. The accumulation of cells thickens the CIMT further, and activates the endothelium, resulting in severer disturbance to the homeostasis on blood-tissue interface, and eventually leading to plaque(7–9).

The composition of CP is largely associated with the risk of stroke of patients. Advanced lesion may give rise to the thrombus, which could occlude the blood vessel. Rupture and erosion of CP may cause emboli, and induce the cerebrovascular events. Therefore, CA with the presence of CP increase the risk of cerebrovascular diseases(8, 10–13).

Clinically, ultrasound, as a non-invasive equipment, is commonly used to evaluate CA by examining the several related parameters (CIMT, carotid stenosis and carotid plaque morphology). However, assessment of carotid plaque textures is not common in routine examinations. Therefore, we aimed to evaluate the degree of CA in post-RT NPC patients and subjects with cardiovascular risk factors (CVRFs) by CIMT and incidence of CP using ultrasonography; and also aimed to investigate the feasibility of using computer-assisted ultrasound to study the difference in carotid plaque characteristics in radiation-induced and non-radiation-induced CA.

Methods

Aim

This study investigated the feasibility of using a computer-assisted method to evaluate and differentiate the carotid plaque characteristics in radiation-induced and non-radiation-induced carotid atherosclerosis.

Subject recruitment

Post-RT NPC patients treated with intensity-modulated radiation therapy were recruited in the Department of Clinical Oncology of Queen Mary Hospital when the patients attended the follow up clinics. The inclusion criteria of post-RT NPC patients were Chinese NPC patients, aged 18 years or above, received a single course of RT for the primary tumour and neck lymph nodes, and a post-RT duration of 4 years or more. The exclusion criteria were a known history of leukopenia, thrombocytopenia, severe hepatic or renal dysfunction, an evidence for inflammatory or other malignant diseases, and a known history of carotid atherosclerosis prior to RT, previous carotid endarterectomy or stenting.

Patients with cardiovascular risk factor (CVRF) were recruited by poster advertisement in the Hong Kong Polytechnic University. The inclusion criteria of CVRF subjects were Chinese, older than 40 years, and have at least one CVRF, namely smoking, diabetes mellitus, hypertension, hypercholesterolemia or heart disease. The criteria for identifying these CVRF were the same as described in our previous study(14). The exclusion criteria for the recruitment of patients were previous RT, carotid endarterectomy or stenting.

Study design and ultrasound examination

The Human Subject Ethics Subcommittee of the Hong Kong Polytechnic University (HSEARS20160930001) and the Institutional Review Board of the University of Hong Kong/Hospital Authority Hong Kong West Cluster approved this study (HA RE001F3). Each participant was provided an information sheet with detailed information of the study and the rights of participants. Informed written consent form was obtained from all participants before the commencement of the examinations. Medical history of the post-RT NPC patients including post-RT duration, history of chemotherapy and atherosclerotic diseases was obtained from archived clinical records of the patients. Individual face-to-face interview was conducted with post-RT NPC patients and CVRF patients to obtain the demographical information and history of CVRF.

All recruited participants had a carotid ultrasound examination. All ultrasound examinations were performed using the Esaote MyLab™ Twice eHD CrystaLine ultrasound unit in conjunction with a 3–13 MHz linear transducer (Esaote, Genoa, Italy). In order to ensure measurements were obtained with the subjects at resting state, all subjects were allowed to rest for at least 10 minutes before the ultrasound examination. In the carotid ultrasound examination, the subject lay supine on the examination couch with the shoulders and neck supported by a pillow so that the neck was slightly extended and the head turned away from the side under examination. On each side of the neck, the CIMT was evaluated using the automated quantification programs of the ultrasound unit: radiofrequency-based quality intima-media thickness (RF-QIMT).

For each subject, the presence or absence of carotid plaque in the internal, external and common carotid arteries was assessed. Carotid plaque was identified as focal arterial wall thickening > 50% of the adjacent intima-media layer(15). All identified carotid plaque of each subject were included in the study, and the characteristics of each carotid plaque were evaluated for grey-scale median (GSM) and detailed plaque texture analysis (DPTA).

In the evaluation of GSM and DPTA, multiple longitudinal grey scale ultrasound images of the carotid plaque were obtained. Archived digital images were reviewed and analysed using image-processing software (Adobe Photoshop CS v.8.0, Adobe, San Jose, CA, United States; and Image Pro Plus v.6.0, Media Cybernetics, Rockville, MD, United States).

For each carotid plaque, five longitudinal sonograms which clearly demonstrating the borders and internal echotexture of the plaque were selected to evaluate the GSM and DPTA. Image normalization was performed before the evaluations. With the use of the histogram facility of the software (Adobe Photoshop CS, v.8.0, Adobe, San Jose, CA, United States), the grey scale value of two reference areas (blood and adventitia) in the image were standardised 0 for blood and 190 for adventitia. All the pixels of the image were adjusted accordingly based on the standard linear scale, and a normalized image was produced.

For the evaluation of GSM, the carotid plaque was outlined manually on the normalized grey scale ultrasound image using software Adobe Photoshop CS, v.8.0 (Adobe, San Jose, CA, United States) and

then the software calculated the median of the grey scale value of pixels (i.e. GSM) within the region of interest (ROI).

For the DPTA, the software Image Pro Plus v.6.0 (Media Cybernetics, Rockville, MD, United States) was used to analyse the normalized grey scale ultrasound images. In this software, 4-connect pixels consist in an “object”, and numbers of objects with defined grey scale ranges consist in a component. In the image analysis, the different components of carotid plaque were color-coded by the software based on the different grey scale ranges: yellow for blood (grey scale ranges 0–9), orange for lipid (10–31), red for muscle (32–74), light blue for fibrous tissue (75–111) and dark blue for calcium (112–255). The blood, lipid and muscle appeared hypoechoic, while fibrous tissue and calcification were hyperechoic(16). For each carotid plaque component, the average pixel density, area percentage and integrated optical density (IOD) were evaluated. Average pixel density was the mean value of pixel densities of each component. Area percentage was the percentage that the area of each component relative to the area of the plaque. IOD was the product of area and average pixel density, and it represented the integration of pixel density of the plaque component.

Data analysis

Basic information of the subjects and plaque characteristics were expressed as mean ± SD or SEM for the continuous data; counts and percentage were presented for categorical data. Normal distribution of the data was evaluated by Shapiro-Wilk test. The difference between post-RT NPC group and CVRF group were evaluated using Mann Whitney U tests for nonparametric variables (plaque number per subject, CIMT and GSM), unpaired Student t-test for parametric variables (age), and chi-square tests for categorical data (CVRFs, number of CVRFs, plaque presence). Comparisons among groups were evaluated by one-way ANOVA. The effects of age, gender, number of CVRFs and exposure to radiation on carotid plaque characteristics were analysed by multiple linear regression models. The risk factors regarded as candidate variables were age, gender, number of CVRFs and radiation. We used multivariable model to analyse the effects of different risk factors on plaque characteristics (CIMT, plaque presence, number of plaques per subject, plaque components). All statistical analyses were performed using SPSS 22 (IBM Corporation, Armonk, NY, United States) and Prism 7.0 (GraphPad Software, San Diego, CA, United States). P value < 0.05 was considered to be significant.

Results

Demographical information

From April 2017 to May 2018, we recruited 111 post-RT NPC and 110 CVRF subjects. However, 4 post-RT patients were excluded, as 2 of them lacked comprehensive clinical data and the other 2 were unsatisfied to the inclusion criteria. Eventually, 107 post-RT NPC and 110 CVRF subjects were analysed in the study. The demographic and clinical information of the subjects are summarized in Table 1. The subjects in two groups were similarly aged (58.4 ± 1.1 vs. 60.7 ± 0.7, $p > 0.05$), but with different gender ratio. There were significantly more male subjects in post-RT NPC group than CVRF group (68/107 vs. 44/110, $p < 0.001$).

Amongst the post-RT NPC group, 57 subjects (53.3%) had no CVRFs, 31 (29.0%) had one CVRF and 19 (17.8%) had more than one CVRFs.

In CVRF group, 58 of them (52.7%) had only one CVRF, while the remainder had at least two CVRFs (52, 47.3%). The most prevalent CVRF was hypertension (74, 67.3%), followed by hyperlipidaemia (69, 62.7%), diabetes (23, 20.9%) and cigarettes (9, 8.2%).

CIMT assessment

As shown in Supplemental Figure I and Table 2, post-RT NPC patients had higher CIMT (748 ± 15.1 μm) than CVRF subjects (680 ± 10.0 μm, p^T=0.001). Besides, both post-RT NPC patients with CVRFs (740.4 ± 20.0 μm) and without CVRFs (756.7 ± 23.0 μm) had greater CIMT than CVRF subjects (680 ± 10.03 μm, p^M=0.004).

Carotid plaque assessment

Post-RT NPC subjects were prone to have plaques compared to CVRF subjects (80.4% vs. 38.2%, p^T<0.001), and had larger quantities (2.3 ± 0.2 vs. 0.5 ± 0.1, p^T<0.001). Both post-RT NPC patients with/without CVRFs had more plaques (2.6 ± 0.3/2.0 ± 0.2, p^M<0.001) than CVRF group (Table 2).

However, no significant difference of GSM was found between post-RT NPC and CVRF subjects (p^T>0.05), neither between post-RT NPC patients with/without CVRFs and CVRF group (p^M>0.05).

Detailed plaque components assessment

The frequency of presence of different components within a plaque is shown in Supplemental Table I and Table II. Plaque components were further evaluated through average pixel density, area percentage and IOD. Differences were analysed between post-RT NPC patients and CVRF subjects, and among the groups of post-RT NPC patients with/without CVRFs and CVRF (Table 3).

There was no significant difference in the average pixel density of the five plaque components between post-RT NPC and CVRF groups (p^T>0.05).

The plaques of CVRF subjects were found to have more lipid and less calcification (Fig. 1, Table 3) with larger area of lipid (46.3 ± 17.9%), compared to total post-RT NPC patients (42.1 ± 16.9%, p^T=0.034) and post-RT NPC patients having CVRF (40.5 ± 16.1%; p^M=0.020). Conversely, plaques of CVRF subjects had significantly less amount of calcification (3.0 ± 5.7%) compared to post-RT NPC patients (4.8 ± 7.7%, p^T=0.012) and post-RT NPC patients with CVRF (4.4 ± 6.6%, p^M=0.030). No significant differences were found between post-RT NPC and CVRF subjects in the area percentage of blood, muscle and fibrous tissue inside a plaque (p > 0.05).

IOD representing the product of pixel density and area of plaque component, the total post-RT NPC patients had significantly higher IOD than CVRF subjects in both muscle (3086 ± 3121 vs. 2392.0 ± 1911.0, p^T=0.043) and calcification (4073 ± 6667 vs. 2675 ± 6615, p^T=0.007) (Table 3). CPs of post-RT

NPC patients with CVRF had significantly higher IOD of muscle (3416 ± 3106), compared to post-RT NPC patients without CVRF (2712 ± 3108, p = 0.025) and CVRF subjects (2392 ± 1911, p = 0.012) (p^M=0.004). Additionally, CPs of post-RT NPC patients with CVRF had significantly higher IOD of calcification (3767 ± 5593) than CVRF subjects (2675 ± 6615, p^M=0.018).

Relationship of plaque features and various risk factors

Table 4 summarises the effects of various risk factors on atherosclerosis related parameters. Post-RT NPC patients were further divided into three subgroups (0 CVRF, 1 CVRF and ≥ 2 CVRFs). After adjustment of age and gender, results showed that age and radiation were significantly associated with CIMT, presence of plaque and the number of plaque ($p \leq 0.001$). Number of CVRFs were significantly associated with CIMT and number of plaques ($p < 0.05$). The aging subjects tended to have higher CIMT(r = 0.36; [95% CI: 0.23 to 0.47]) and larger number of plaques (r = 0.25; [95% CI: 0.12 to 0.37], data not show).

Among the mentioned risk factors, age played the most significant role on lipid and calcification area of a plaque (Table 5, $p < 0.001$) in an opposite trend. Advancing age was associated with less lipidic area (r=-0.27; 95% CI [-0.43 to -0.10]), but more calcific area (r=-0.29; 95% CI [0.12 to 0.44], data not show). Additionally, radiation exerted significantly import influence on IOD of muscle (p = 0.046), by radiation-induced plaques having higher IOD value than non-radiation-induced plaques (Table 5).

However, the results indicated none of the risk factors played statistically significant role on IOD of calcification (Table 5. P value of age, gender, number of CVRFs, radiation were 0.064, 0.190, 0.143, 0.536 respectively).

Discussion

We investigated the difference in CIMT and carotid plaque components of radiation-induced and non-radiation-induced. To unveil the plaque components characteristics, we used computer-assisted method to assess the plaque GSM and DPTA. We also investigated the effects of several risk factors on plaque components. The major findings of this study are as follows:

(a) Radiation-induced CA leads to higher CIMT, and is more likely to develop CPs than non-radiation-induced CA; (b) No significant difference of GSM was found between radiation-induced and non-radiation-induced CPs; (c) DPTA indicates radiation-induced CPs tend to have more calcification, while non-radiation-induced plaques are more lipid-rich and thus are more unstable; (d) The plaque constituents are mainly effected by age and exposure to the radiation.

CIMT and incidence of plaque formation

CIMT and incidence of carotid plaque reflected the degree of CA of patients. Much severer CA was identified with higher CIMT and more incidence of plaque formation. Few studies compared the plaque

burden between radiation-induced atherosclerosis and spontaneous atherosclerosis caused by CVRFs. Our group previously reported that no significantly difference in CIMT existed in radiation-induced carotid atherosclerosis (post-RT NPC patients) compared to non-radiation-induced CA (diabetes patients without RT) (p_{cor}=0.732), and higher CIMT was associated to male gender (p_{cor}<0.01) and advanced age (p_{cor}<0.01)(12). In present study, radiation-induced atherosclerosis was with a higher CIMT and more plaque numbers. Besides, radiation-induced atherosclerosis with or without the presence of CVRFs had a higher CIMT and more plaques, compared to non-radiation-induced atherosclerosis. Further investigation found that number of CVRFs and radiation had significant influence on CIMT and the number of plaques. Therefore, radiation played a dominate role in carotid wall thickening and progressing the atherosclerosis, which was consistent with previous study(17).

The underlying causes could be explored from the biological responses of endothelial cells to ionizing radiation. CIMT and plaque formation was the consequences of cell injury by radiation. Exposure to the ionizing radiation caused DNA double strands damage of endothelial cells. When DNA damage repair could not suppress the damage, the constant injury accumulated and induced the expression of adhesion molecules, then promoting the atherosclerosis by facilitating the circulating immune cells anchoring on the endothelium, and resulting the advanced atherosclerosis through inflammation, cell apoptosis, proliferation and fibrosis (12, 18).

Evaluation of carotid plaque components

The stability of the plaque could partly be decided through plaque composition. Hypoechoic plaques were more vulnerable plaques, being more unstable and having higher association with cerebrovascular events. Carotid plaque rupture is higher associated with the components of the plaque. Vulnerable plaques are characterized by larger volume, slim cap with lipid-rich necrosis core inside and highly inflammatory(19–21). Therefore, assessing the plaque components could evaluate the plaque vulnerability and help treatment planning.

GSM is a common assessment for the overall plaque echogenicity for detecting plaque vulnerability, but it is limited in distinguishing different plaque components within a plaque by its first-order statistic value(22). Thus, to evaluate plaque vulnerability by the detailed plaque texture, GSM is more commonly used in conjunction with other parameters such as degree of carotid artery stenosis and CIMT(11, 23–25). A previous study demonstrated that there was no significant difference in GSM between radiation-induced plaques and non-radiation-induced plaques(11). Result of the present study was consistent with the previous one. We found that the GSM of radiation-induced and non-radiation-induced CPs was not significantly different. Therefore, a DPTA was conducted in the present study subsequently to evaluate the plaque composition in detail.

Numerous studies have reported various imaging techniques applying in plaque components analysis. Magnetic resonance imaging (MRI) is a robust imaging tool for soft tissue examination and has been used for evaluation of plaque composition(26–28). Intravascular ultrasound (IVUS) elastography(29, 30) and acoustic radiation force impulse (ARFI) elastography ultrasound(31, 32) can be used to estimate the

plaque stiffness and assess the plaque composition in a recent study based on the plaque mechanical properties. Multi-detector computed tomography angiography (CTA) can assess plaque composition with high sensitivities and inter-observer agreements(33–35). Meanwhile, some drawbacks should be aware in these imaging modalities. MRI is not suitable for patients with metal implants or pacemakers. It is costly in both expenses and time-consume. IVUS is an invasive procedure and the study of ARFI for investigating the plaque composition is conducted on 4 patients in a pilot study. Thus, it is emerging, but without solid evidences at this stage. CTA cannot distinguish intra-plaque haemorrhage and lipids, and the examination involves radiation and administration of iodinated contrast agent which is not suitable for patients with deteriorated renal function(21).

The first application of ultrasound to investigate plaque constituents preoperatively was reported in 1980's(36). The study applied ultrasonography to classify the plaques as heterogeneous or homogeneous and compared the ultrasound images with pathological findings. Lai et al.(37) assessed the plaque constituents by analysing the pixel distribution of B-mode ultrasound imaging. They found that the pixel distribution of the ultrasound image was highly correlation with the result of histological sections ($r = 0.53–0.86$, 95% CI [0.03–0.92], $p < 0.05$). They set different pixel ranges according to pathologic findings and applied the digital DPTA as an additional analysis combined with GSM in this study. Subsequently, a Polish research group utilized the DPTA and find it was highly consistent with visual assessment and histologic findings and effective in predicting neurological complications through detecting microembolism(16). Therefore, computer-aided DPTA could be an efficient method to assess plaque vulnerability. Based on this, computer-aided DPTA was adopted to compare the plaque composition characteristics between radiation-induced and non-radiation-induced atherosclerosis in this study.

In the DPTA of CPs in the present study, more radiation-induced plaques have calcification than non-radiation-induced plaques, and radiation-induced plaque tend to be more hyperechoic. Compared with hypoechoic plaques in non-radiation-induced group, radiation-induced plaques are less vulnerable with larger area of calcification. The results are consistent with the study of Fokkema et al. in which they used MRI and found that radiation-induced carotid lesions were less inflammatory with more fibrosis tissue(38, 39). Toprak's groups found the soft and dense present plaques turned calcified after receiving radiotherapy in head and neck cancer patients(40). Similar studies also reported that microcalcifications(41), cardiovascular calcifications(42), calcification in basal ganglia(43) and cerebral calcification(44) could be found in thoracic and cranial cancer patients after therapeutic radiation.

The causes of radiation-induced atherosclerosis with more calcifications may be resulted from the serial responses of mesenchymal stem cells (MSC) after ionizing radiation. Radiation induces excessive oxidative stress in the microenvironment of carotid vessel and induced the endothelial dysfunction, which could create the cross-talk with MSC. When MSCs are exposed in an oxidative surroundings, necrosis and apoptosis are being induced. Besides, its extreme low survivability makes it difficult to recover by stem cell therapy. Then, dead MSCs exert the residual influence on vascular calcification to propel the progress constantly. Moreover, the differentiation of MSCs can be affected by the interacted cells. Under the

progress of atherosclerosis, the existed osteo-like cells could induce the MSCs to differentiate into calcified vascular smooth muscle cells, which attenuate the further vascular calcification. Although the conditioned medium of MSCs plays the protective role by anti-inflammation, anti-apoptosis, regulating the Wnt signal in a negative way and inhibiting the combination of BMP2 signal(45), the excessive oxidative stress could still trigger the amplified atherosclerosis responses. Massive pathological cells are recruited at the focal and release various inflammatory factors to disturb the original medium created by MSCs alone. The mentioned reasons may be the potential biological mechanism of radiation-induced CPs showing more calcification compared to the non-radiation-induced ones.

Limitations

This study was a retrospective study. Further prospective studies should be conducted to investigate the value of the present DPTA method in predicting the stroke risk of the post-RT NPC patients and CVRF subjects. Secondly, based on the sample size of this study, the observed power of radiation (0.358) and gender (0.172) are less than 0.6 in multivariate models, which may influence the statistical results. Further studies with a larger sample size are suggested.

Conclusions

Though radiation-induced CPs are more prevalent, non-radiation-induced plaques have more lipid than radiation-induced plaques. Considering both CA burden and plaque component, both post-RT NPC patients and individuals with CVRF have a high risk of cerebrovascular diseases. Ultrasound aided by computer is a deserved-considered modality for population, with the priority of non-invasive, inexpensive, timesaving and informative for plaque texture analysis.

Abbreviations

CA=carotid atherosclerosis

CIMT=carotid intima-media thickness

CP=Carotid plaque

CVRF=cardiovascular risk factor

DPTA=detailed plaque texture analysis

GSM=grey-scale median

IOD=integrated of density

MSC=mesenchymal stem cells

NPC= nasopharyngeal carcinoma

RT=radiotherapy

Declarations

Ethics approval and consent to participate

The Human Subject Ethics Subcommittee of the Hong Kong Polytechnic University (HSEARS20160930001) and the Institutional Review Board of the University of Hong Kong/Hospital Authority Hong Kong West Cluster approved this study (HA RE001F3). Each participant was provided an information sheet with detailed information of the study and the rights of participants. Informed written consent form was obtained from all participants before the commencement of the examinations.

Consent for publication

All authors have read and approved the submitted manuscript for publication. The manuscript has not been submitted elsewhere nor published elsewhere in whole or in part, except as an abstract (if relevant).

Availability of data and materials

The datasets used and analysed during the current study are available from the corresponding author on reasonable request.

Competing interests

The authors declare that they have no competing interests.

Sources of funding

This study was supported by a research studentship (RUAS) and a research grant (P0008624, UAB9) of the Hong Kong Polytechnic University.

Author's contributions

Yuanxi Li contributed to the study conception and design, collection, analysis and interpretation of data and a major contributor in writing the manuscript. Michael TC Ying is the corresponding author of the manuscript, and contributed to study conception and design, critical revision of the manuscript for the important intellectual contents, and final approval of the manuscript. Dora LW Kwong and Vincent WC Wu contributed to the data collection, and critical revision of the manuscript for the important intellectual contents. Shea Ping Yip, Helen KW Law and Shara WY Lee contributed to the critical revision of the manuscript for the important intellectual contents.

Acknowledgement

We thank the assistance of the staff in the Department of Clinical Oncology, Queen Mary Hospital.

Author's information

a. Department of Health Technology and Informatics, The Hong Kong Polytechnic University, Hong Kong SAR, China
b. Department of Clinical Oncology, The University of Hong Kong, Queen Mary Hospital, Hong Kong SAR, China

References

1. Bray F, Ferlay J, Soerjomataram I, Siegel RL, Torre LA, Jemal A. Global cancer statistics 2018: GLOBOCAN estimates of incidence and mortality worldwide for 36 cancers in 185 countries. CA Cancer J Clin. 2018;68(6):394-424.
2. Lee AW, Ma BB, Ng WT, Chan AT. Management of Nasopharyngeal Carcinoma: Current Practice and Future Perspective. J Clin Oncol. 2015;33(29):3356-64.
3. Leung TW, Tung SY, Sze WK, Wong FC, Yuen KK, Lui CM, et al. Treatment results of 1070 patients with nasopharyngeal carcinoma: an analysis of survival and failure patterns. Head Neck. 2005;27(7):555-65.
4. Glastonbury CM. Nasopharyngeal carcinoma: the role of magnetic resonance imaging in diagnosis, staging, treatment, and follow-up. Top Magn Reson Imaging. 2007;18(4):225-35.
5. Touboul PJ, Hernandez-Hernandez R, Kucukoglu S, Woo KS, Vicaut E, Labreuche J, et al. Carotid artery intima media thickness, plaque and Framingham cardiovascular score in Asia, Africa/Middle East and Latin America: the PARC-AALA study. Int J Cardiovasc Imaging. 2007;23(5):557-67.
6. Naqvi TZ, Lee MS. Carotid intima-media thickness and plaque in cardiovascular risk assessment. JACC Cardiovasc Imaging. 2014;7(10):1025-38.
7. Ross R. Atherosclerosis–an inflammatory disease. N Engl J Med. 1999;340(2):115-26.
8. Lusis AJ. Atherosclerosis. Nature. 2000;407(6801):233-41.
9. Sumpio BE, Riley JT, Dardik A. Cells in focus: endothelial cell. Int J Biochem Cell Biol. 2002;34(12):1508-12.
10. Lam WW, Leung SF, So NM, Wong KS, Liu KH, Ku PK, et al. Incidence of carotid stenosis in nasopharyngeal carcinoma patients after radiotherapy. Cancer. 2001;92(9):2357-63.
11. Cheng SW, Ting AC, Wu LL. Ultrasonic analysis of plaque characteristics and intimal-medial thickness in radiation-induced atherosclerotic carotid arteries. Eur J Vasc Endovasc Surg. 2002;24(6):499-504.
12. Yuan C, Wu VW, Yip SP, Kwong DL, Ying M. Ultrasound Evaluation of Carotid Atherosclerosis in Post-Radiotherapy Nasopharyngeal Carcinoma Patients, Type 2 Diabetics, and Healthy Controls. Ultraschall Med. 2017;38(2):190-7.
13. Stein JH, Korcarz CE, Hurst RT, Lonn E, Kendall CB, Mohler ER, et al. Use of carotid ultrasound to identify subclinical vascular disease and evaluate cardiovascular disease risk: a consensus

statement from the American Society of Echocardiography Carotid Intima-Media Thickness Task Force. Endorsed by the Society for Vascular Medicine. J Am Soc Echocardiogr. 2008;21(2):93-111; quiz 89-90.

14. Yuan C, Wu VW, Yip SP, Kwong DL, Ying M. Predictors of the extent of carotid atherosclerosis in patients treated with radiotherapy for nasopharyngeal carcinoma. PLoS One. 2014;9(12):e116284.
15. Touboul PJ, Hennerici MG, Meairs S, Adams H, Amarenco P, Bornstein N, et al. Mannheim carotid intima-media thickness and plaque consensus (2004-2006-2011). An update on behalf of the advisory board of the 3rd, 4th and 5th watching the risk symposia, at the 13th, 15th and 20th European Stroke Conferences, Mannheim, Germany, 2004, Brussels, Belgium, 2006, and Hamburg, Germany, 2011. Cerebrovasc Dis. 2012;34(4):290-6.
16. Madycki G, Staszkiewicz W, Gabrusiewicz A. Carotid plaque texture analysis can predict the incidence of silent brain infarcts among patients undergoing carotid endarterectomy. Eur J Vasc Endovasc Surg. 2006;31(4):373-80.
17. Gujral DM, Shah BN, Chahal NS, Bhattacharyya S, Hooper J, Senior R, et al. Carotid intima-medial thickness as a marker of radiation-induced carotid atherosclerosis. Radiother Oncol. 2016;118(2):323-9.
18. Gray K, Bennett M. Role of DNA damage in atherosclerosis–bystander or participant? Biochem Pharmacol. 2011;82(7):693-700.
19. Carr S, Farb A, Pearce WH, Virmani R, Yao JS. Atherosclerotic plaque rupture in symptomatic carotid artery stenosis. J Vasc Surg. 1996;23(5):755-65; discussion 65-6.
20. Bentzon JF, Otsuka F, Virmani R, Falk E. Mechanisms of plaque formation and rupture. Circ Res. 2014;114(12):1852-66.
21. Naim C, Douziech M, Therasse E, Robillard P, Giroux MF, Arsenault F, et al. Vulnerable atherosclerotic carotid plaque evaluation by ultrasound, computed tomography angiography, and magnetic resonance imaging: an overview. Can Assoc Radiol J. 2014;65(3):275-86.
22. Elatrozy T, Nicolaides A, Tegos T, Zarka AZ, Griffin M, Sabetai M. The effect of B-mode ultrasonic image standardisation on the echodensity of symptomatic and asymptomatic carotid bifurcation plaques. Int Angiol. 1998;17(3):179-86.
23. Biasi GM, Sampaolo A, Mingazzini P, De Amicis P, El-Barghouty N, Nicolaides AN. Computer analysis of ultrasonic plaque echolucency in identifying high risk carotid bifurcation lesions. Eur J Vasc Endovasc Surg. 1999;17(6):476-9.
24. Martinez-Sanchez P, Fernandez-Dominguez J, Ruiz-Ares G, Fuentes B, Alexandrov AV, Diez-Tejedor E. Changes in carotid plaque echogenicity with time since the stroke onset: an early marker of plaque remodeling? Ultrasound Med Biol. 2012;38(2):231-7.
25. Ibrahimi P, Jashari F, Johansson E, Gronlund C, Bajraktari G, Wester P, et al. Common carotid intima-media features determine distal disease phenotype and vulnerability in asymptomatic patients. Int J Cardiol. 2015;196:22-8.

26. Kerwin WS, O'Brien KD, Ferguson MS, Polissar N, Hatsukami TS, Yuan C. Inflammation in carotid atherosclerotic plaque: a dynamic contrast-enhanced MR imaging study. Radiology. 2006;241(2):459-68.
27. Sun J, Canton G, Balu N, Hippe DS, Xu D, Liu J, et al. Blood Pressure Is a Major Modifiable Risk Factor Implicated in Pathogenesis of Intraplaque Hemorrhage: An In Vivo Magnetic Resonance Imaging Study. Arterioscler Thromb Vasc Biol. 2016;36(4):743-9.
28. Lin R, Chen S, Liu G, Xue Y, Zhao X. Association Between Carotid Atherosclerotic Plaque Calcification and Intraplaque Hemorrhage: A Magnetic Resonance Imaging Study. Arterioscler Thromb Vasc Biol. 2017;37(6):1228-33.
29. de Korte CL, Pasterkamp G, van der Steen AF, Woutman HA, Bom N. Characterization of plaque components with intravascular ultrasound elastography in human femoral and coronary arteries in vitro. Circulation. 2000;102(6):617-23.
30. de Korte CL, van der Steen AF, Cepedes EI, Pasterkamp G, Carlier SG, Mastik F, et al. Characterization of plaque components and vulnerability with intravascular ultrasound elastography. Phys Med Biol. 2000;45(6):1465-75.
31. Czernuszewicz TJ, Homeister JW, Caughey MC, Farber MA, Fulton JJ, Ford PF, et al. Non-invasive in vivo characterization of human carotid plaques with acoustic radiation force impulse ultrasound: comparison with histology after endarterectomy. Ultrasound Med Biol. 2015;41(3):685-97.
32. Allen JD, Ham KL, Dumont DM, Sileshi B, Trahey GE, Dahl JJ. The development and potential of acoustic radiation force impulse (ARFI) imaging for carotid artery plaque characterization. Vasc Med. 2011;16(4):302-11.
33. Das M, Braunschweig T, Muhlenbruch G, Mahnken AH, Krings T, Langer S, et al. Carotid plaque analysis: comparison of dual-source computed tomography (CT) findings and histopathological correlation. Eur J Vasc Endovasc Surg. 2009;38(1):14-9.
34. Ajduk M, Pavic L, Bulimbasic S, Sarlija M, Pavic P, Patrlj L, et al. Multidetector-row computed tomography in evaluation of atherosclerotic carotid plaques complicated with intraplaque hemorrhage. Ann Vasc Surg. 2009;23(2):186-93.
35. Nikolaou K, Becker CR, Muders M, Babaryka G, Scheidler J, Flohr T, et al. Multidetector-row computed tomography and magnetic resonance imaging of atherosclerotic lesions in human ex vivo coronary arteries. Atherosclerosis. 2004;174(2):243-52.
36. Reilly LM, Lusby RJ, Hughes L, Ferrell LD, Stoney RJ, Ehrenfeld WK. Carotid plaque histology using real-time ultrasonography. Clinical and therapeutic implications. Am J Surg. 1983;146(2):188-93.
37. Lal BK, Hobson RW, 2nd, Pappas PJ, Kubicka R, Hameed M, Chakhtoura EY, et al. Pixel distribution analysis of B-mode ultrasound scan images predicts histologic features of atherosclerotic carotid plaques. J Vasc Surg. 2002;35(6):1210-7.
38. Fokkema M, den Hartog AG, van Lammeren GW, Bots ML, Pasterkamp G, Vink A, et al. Radiation-induced carotid stenotic lesions have a more stable phenotype than de novo atherosclerotic plaques. Eur J Vasc Endovasc Surg. 2012;43(6):643-8.

39. Pletsch-Borba L, Selwaness M, van der Lugt A, Hofman A, Franco OH, Vernooij MW. Change in Carotid Plaque Components: A 4-Year Follow-Up Study With Serial MR Imaging. JACC Cardiovasc Imaging. 2018;11(2 Pt 1):184-92.
40. Toprak U, Aytas I, Ustuner E, Habiboglu R, Aslan N, Pasaoglu E, et al. Sonographic assessment of acute changes in plaque size and echogenicity and in intima-media thickness of carotid arteries after neck radiation therapy. J Clin Ultrasound. 2012;40(9):566-71.
41. Rebner M, Pennes DR, Adler DD, Helvie MA, Lichter AS. Breast microcalcifications after lumpectomy and radiation therapy. Radiology. 1989;170(3 Pt 1):691-3.
42. Apter S, Shemesh J, Raanani P, Portnoy O, Thaler M, Zissin R, et al. Cardiovascular calcifications after radiation therapy for Hodgkin lymphoma: computed tomography detection and clinical correlation. Coron Artery Dis. 2006;17(2):145-51.
43. Harwood-Nash DC, Reilly BJ. Calcification of the basal ganglia following radiation therapy. Am J Roentgenol Radium Ther Nucl Med. 1970;108(2):392-5.
44. Suzuki S, Nishio S, Takata K, Morioka T, Fukui M. Radiation-induced brain calcification: paradoxical high signal intensity in T1-weighted MR images. Acta Neurochir (Wien). 2000;142(7):801-4.
45. Xie C, Ouyang L, Chen J, Zhang H, Luo P, Wang J, et al. The Emerging Role of Mesenchymal Stem Cells in Vascular Calcification. Stem Cells Int. 2019;2019:2875189.

Tables

Table 1. Basic information of the study subjects

	post-RT NPC (n=107)	CVRF (n=110)	P Value
Age, yrs	58.4 ± 1.1	60.7 ± 0.7	0.069
Gender(female/male), n	39/68	66/44	<0.001***
Chemotherapy, n (%)	59 (55.1)	-	-
Post-RT Duration	15 ± 8.9	-	-
Number of CV† risk factors			
0, n (%)	57(53.3)	-	-
1, n (%)	31(29.0)	58(52.7)	<0.001***
≥2, n (%)	19(17.8)	52(47.3)	<0.001***
CV risk factors			
Hypertension, n (%)	40 (37.4)	74 (67.3)	<0.001***
Hyperlipidaemia, n (%)	17 (15.9)	69 (62.7)	<0.001***
Diabetes, n (%)	6 (5.6)	23 (20.9)	<0.001***
Current Smoking, n (%)	6 (5.6)	9 (8.2)	0.455
Heart disease, n (%)	4 (3.7)	-	0.041*

Values are expressed as mean ± SD;

†CV=cardiovascular; yrs=years

*P<0.05, ** P<0.01, ***P<0.001

Table 2. Plaque characteristics comparison in radiation-induced and non-radiation-induced carotid plaques

	Total	post-RT NPC (1) With CVRFs	(2) Without CVRFs	(3) CVRF	P^T	P^M	*Dunnett Post-hoc*
CIMT(μm), N	748.0 ± 15.1 N=107	740.4 ± 20.0, N=50	756.7 ± 23.0, N=57	680.4 ± 10.0, N=110	0.001***	0.004**	1□3*; 2□3*
Number of the subject with Plaque (%), N†	86 (80.4), N=107	-	-	42(38.2), N=110	<0.001***	-	-
Plaque numbers Per subject, N	2.3 ± 0.2, N=107	2.6 ± 0.3, N=50	2.0 ± 0.2, N=57	0.5 ± 0.1, N=110	<0.001***	<0.001***	1□3*** 2□3***
GSM of plaque, n	9.1 ± 18.0, n=247	28.7 ± 16.7, n=131	29.6 ± 19.4, n=116	25.5 ± 15.0, n=59	0.087	0.229	-

Values are mean ± SEM

†N = total number of subject in the corresponding analysis; n = total number of carotid plaque in the corresponding analysis; GSM=grey-scale median

P^T=Comparison between total post-RT NPC subjects and CVRF subjects.

P^M=Multiple comparison among post-RT NPC subjects with CVRFs, without CVRFs and CVRF subjects.

*P<0.05, ** P<0.01, ***P<0.001

Table 3. Difference of plaque component characteristics between post-RT NPC group and CVRF group

Component	Post-RT NPC(n=247)			CVRF (n=59)	P value[T]	Pvalue[M]	*Dunnett Post-hoc*
	Total	1. with CVRFs (n=131)	1. without CVRFs (n=116)	(3)			
Average pixel density							
blood	7.5 ± 2.9	7.8 ± 3.9	7.2 ± 0.8	7.3 ± 1.0	0.316	0.160	-
lipid	22.1 ± 3.7	22.3 ± 4.0	21.9 ± 3.5	21.4 ± 4.5	0.432	0.259	-
muscle	44.6 ± 6.4	44.8 ± 6.5	44.4 ± 6.4	43.2 ± 6.4	0.072	0.167	-
fibrous tissue	86.6 ± 4.1	86.6 ± 3.8	86.5 ± 4.4	86.5 ± 4.7	0.973	0.994	-
calcification	129.5 ± 11.8	128.3 ± 10.6	131.0 ± 13.0	130.2 ± 13.36	0.851	0.432	-
Area percentage (%)							
blood	14.8 ± 14.1	15.9 ± 15.2	13.6 ± 12.8	15.0 ± 13.4	0.720	0.160	-
lipid	42.1 ± 16. 9	40.5 ± 16.1	43.8 ± 17.8	46.3 ± 17.9	0.034*	0.259	-
muscle	31.0 ± 13.4	31.3 ± 13.5	30.6 ± 13.4	29.2 ± 15.3	0.249	0.167	-
fibrous tissue	7.4 ± 7.6	7.8 ± 8.1	6.9 ± 7.1	6.6 ± 8.3	0.176	0.994	-
calcification	4.8 ± 7.7	4.4 ± 6.6	5.1 ± 8.8	3.0 ± 5.7	0.012*	0.432	-
IOD							
blood	224.4 ± 938.0	313.2 ± 1276.0	124.1 ± 148.1	143.3 ± 197.4	0.802	0.194	-
lipid	1986.0 ± 2157.0	1503.0 ± 1097.0	1581.0 ± 1171.0	2056.0 ± 1967.0	0.498	0.966	-
muscle	3086.0 ± 3121.0	3416.0 ± 3106.0	2712.0 ± 3108.0	2392.0 ± 1911.0	0.043*	0.004**	1–2*; 1–3**
fibrous tissue	1147.0 ± 1112.0	1299.0 ± 1334.0	975.3 ± 760.0	1090.0 ± 1181.0	0.278	0.065	-
calcification	4073.0 ± 6667.0	3767.0 ± 5593.0	4419.0 ± 7714.0	2675.0 ± 6615.0	0.007**	0.018*	1–3*

Values are presented as mean ± SD. [T]P value = Difference between total post-RT NPC patients and CVRF subjects. [M]P value = Difference among post-RT NPC patients with/without CVRFs VS. CVRF subjects, *P<0.05, **P<0.01.

Table 4. Effects of various risk factors on plaque characteristics by multivariate analysis, with the adjustment of age and gender

	CIMT			Plaque presence			Number of plaque per subject			Overall p value
	Partial η^2(df1,df2)	F	p	Partial η^2(df1,df2)	F	p	Partial η^2(df1,df2)	F	p	
Age	0.181(1,210)	46.510	<0.001***	0.136(1,210)	13.442	<0.001***	0.060(1,210)	33.090	<0.001***	<0.001***
Gender	0.008(1,210)	1.717	0.192	0.004(1,210)	0.935	0.335	0.006(1,210)	1.341	0.248	0.346
Number of CVRFs	0.029(2,210)	3.018	0.048*	0.006(2,210)	0.638	0.529	0.024(2,210)	2.616	0.075	0.025*
Radiation	0.052(1,210)	11.423	0.001**	0.143(1,210)	35.055	<0.001***	0.260(1,210)	73.967	<0.001***	<0.001***

number of CVRFs were grouped by subjects without CVRF, with 1CVRF or ≥2 CVRFs. *P<0.05, ** P<0.01, ***P<0.001

Table 5. Effects of various risk factors on plaque components characteristics by multivariate analysis, with the adjustment of age and gender.

	Area percentage lipid			Area percentage calcification			IOD muscle			IOD calcification		
	Partial η^2	F	P	Partial η^2	F	p	Partial η^2	F	p	Partial η^2	F	p
Age	0.063	20.121	<0.001***	0.056	17.802	<0.001***	0.002	0.625	0.430	0.011	3.448	0.064
Gender	0.001	0.156	0.694	0.003	0.875	0.350	0.004	1.280	0.259	0.006	1.728	0.190
Number of CVRFs	0.006	0.855	0.426	0.005	0.717	0.489	0.014	2.109	0.123	0.013	1.955	0.143
Radiation	0.012	3.699	0.055	0.002	0.750	0.387	0.013	4.012	0.046*	0.001	0.383	0.536

number of CVRFs were grouped by subjects without CVRF, with one CVRF or more than two CVRFs.*P<0.05, ** P<0.01, ***P<0.001

Figures

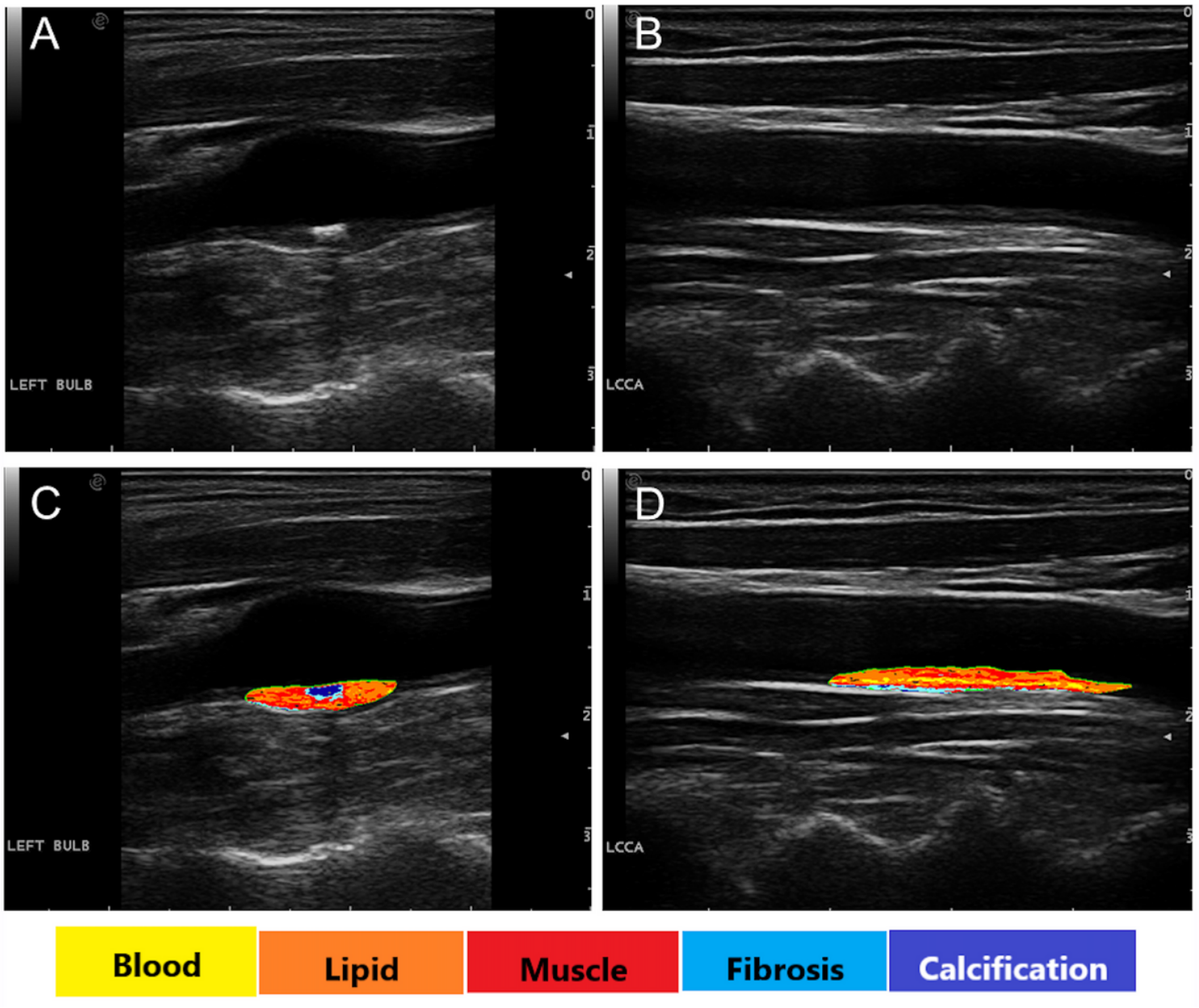

Figure 1

The distribution of different plaque components Longitudinal sonograms show carotid plaques in the carotid bifurcation of a post-RT NPC patient (A) and in the common carotid artery of a CVRF subject (B). Images C and D show the detailed plaque texture analysis of the two carotid plaques. Noted the radiation-induced carotid plaque has more calcification (C) than the non-radiation-induced carotid plaque (D).

Supplementary Files

This is a list of supplementary files associated with this preprint. Click to download.

- CVDSupplementalTables.pdf
- CVDSupplementalFigurelegends.docx

- CVDSupplementalFigureICIMT.tiff